Advances in Textile Engineering

Chapter 6

Through-The-Thickness Composite Reinforcements and their Forming Behaviors

***Hao Shen*[1]*; Peng Wang*[1,2*]*; Xavier Legrand*[2]

[1]*University of Lille, Ensait, Gemtex, Roubaix, France.*

[2]*University of Upper Alsace, Ensisa, Mulhouse, France.*

[*]***Correspondence to: Peng Wang,*** *University of Lille, Ensait, Gemtex, Roubaix, France*

Email: peng.wang@ensait.fr

Abstract

Several common applications for polymer composite laminates reinforced in the through-thickness direction made by the textile processes of 3D weaving, stitching, Z-pinning and tufting are reviewed in this paper. An overview of these reinforcement technologies is given to illustrate their processing principles, benefits, drawbacks and practical applications. On the other hand, preforming is a significant step in the manufacturing of textile-reinforced composites with resin infusion processes. It is important to investigate the various forming behaviors for the through-thickness composite reinforcements in order to control the forming defects which would reduce the mechanical properties of the final composite part. Therefore, the definition of each forming behavior, the measurement approaches and some experimental characterizations for certain Through-Thickness Reinforcements (TTR) are also described.

1. Introduction

Polymer laminates reinforced with a two-dimensional (2D) layered fiber structure have been used with outstanding success in the aeronautic, space and automobile sectors,

owing to their high specific strength. However, a poor delamination resistance and impact damage tolerance due to their low through-thickness strength and fracture toughness restrict the application of 2D laminates in some critical and complex parts, subjected to inter-laminar shear stresses [1,2]. Consequently, in an attempt to overcome these problems and to improve the through-thickness mechanical properties of laminates, considerable attention has been given to the development of polymer laminate composites reinforced in the through-thickness direction. A number of techniques have been developed to obtain the through-thickness composite reinforcements, with the most common being 3D weaving [3–8], stitching [9–12], z-pinning [13–15] and tufting [16]. These techniques are effective in increasing the delamination resistance and impact damage tolerance.

On the other hand, these techniques are especially suitable for textile laminates made from dry fabrics. The manufacturing of thermoset based textile-reinforced composites typically requires the preforming of the dry textile structure and the subsequent matrix infusion with resin transfer molding (RTM) or vacuum processes [17]. During the forming, the textile reinforcement is subjected to complex deformations which can modify the fiber distribution and the fiber volume fraction. Thus, it is important to investigate the forming behaviors (material draw-in, interlayer sliding, punch force, shear angle…), which are linked to the occurrence of forming defects (wrinkling, buckling…) to some extent. These forming defects can affect the quality of the final composite products.

This chapter summarizes the recent manufacturing technologies used to reinforce the textile composite through-thickness by illustrating their processing principles, benefits, drawbacks and practical applications. A general understanding concerning the various forming behaviors which are usually investigated in the subsequent preforming process is also present. Several current study results on the forming behaviors of through-thickness composite reinforcement have been mentioned.

2. TTR Technologies

Several current techniques (3D weaving, stitching, z-pinning and tufting) applied to obtain the Through-Thickness Reinforcements (TTR) are reviewed in the following sections.

2.1. 3D weaving

3D weaving process is a variant of the 2D woven process containing only the X axis (warp) and the Y axis (weft). This process can be produced in a standard weaving looms for 2D laminates with some simple modifications. For 3D woven fabric, more than one layer of fabric is woven at the same time, and binder yarn is inserted and interlaces the warp and weft yarns of different layers during the process. Due to the through-the-thickness binding effect, the delamination resistance enhances the impact performance and damage tolerance of such

material systems [18]. 3D woven composites therefore have far lower cracking rates than 2D laminated composites. On the other hand, an integrated 3D woven structure can be regarded as near-net-shape with considerable thickness. There is no necessity to stack layers to create a part, as the full 3D reinforcement is provided by a single fabric. Thus, manufacturing costs and time can be much reduced.

Commercially available 3D woven interlock fabrics can be generally classified into two main categories according to penetration deepness of the binder [19–24]. One is through-thickness (TT) interlock (Fig.1a, c) referred to a penetration all the way through the thickness, while the other one is called layer-to-layer (LTL) interlock (Fig.1b) in which the binder only holds adjacent layers. Furthermore, the classification can be further divided based on the interlacing angle of the structure. If the interlacing angle between the binder and weft yarns has any value except 90° (Fig.1c), it is regarded as the angle interlock (AI). In other words, if the interlacing angle just equals to 90° (**Figure1a**), this special case is considered as orthogonal interlock (ORT).

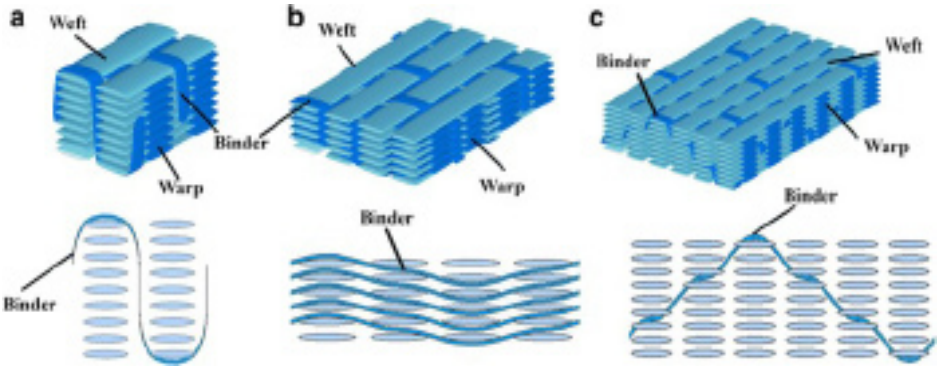

Figure 1: Types of 3D woven composites based on the binder path: (a) ORT, (b) LTL and (c) AI [24]

According to several previous studies [13,25–27], 3D woven fabric has better resistance to interlaminar shear and a larger resistance in the thickness owing to the insertion of binder yarns. In the mechanical testing, the tensile results and flexural results showed that higher modulus and strength can be obtained in the weft direction. In contrast, two main limitations of the process for manufacturing 3D woven composites are the heavy tow weaving and the fiber orientation respectively. Heavy tows more than 24k are difficult to weave using conventional weaving machines [13]. Furthermore, due to the relatively fixed relationship between warp yarns and weft yarns (orthogonal to each other), it is challenging if different orientations for yarns (multiaxial or off-axis fabrics) are needed in the actual production.

The 3D woven composites have been widely used in the industry recently [28,29]. 3D woven AI and LTL architectures have been applied in some places where load transfer is needed around a bend (such as curved beams, T-joints and brackets) [30]. In the automotive industry, the application of 3D woven LTL composites has been also growing fast [31,32]. On the other hand, the ORT woven counterparts also find their own way into the industry. For instance, Bayraktar et al. [31] reported using ORT woven composites to replace high-strength

steel beams. Hemrick et al. [33] reported the use of ORT woven composite in ultra-lightweight heat exchangers in the automotive industry.

2.2. Z-pinning

The Z-pinning technique is developed to reinforce laminate composites in the through-thickness direction to enhance the impact of damage tolerance. One advantage of this process is that it can be applied to increase the strength through-thickness on both dry fabrics and prepreg laminates.

Z-pins act as fine nails that lock the laminate plies together by a combination of friction and adhesion [13]. UAZ® (Ultrasonically Assisted Z-Fiber) is considered to be the most common manufacturing process using the z-pinning technique. It is developed by Aztex Inc. (Waltham, USA) to insert a large number of thin fibrous or metal pins rapidly. Z-pins generally are made of the materials with high stiffness, high strength, such as titanium alloy, steel or fibrous carbon composite, and have a diameter of 0.2-1.0 mm. The detail of the UAZ® process is illustrated in **Figure 2**. A foam carrier is used for the arrangement of z-pins to ensure an even spacing and to offer lateral support during insertion. Using an ultrasonically actuated tool, z-pins can be driven from the foam carrier into the fabric manually or automatically. In the end, the foam carrier needs to be discarded after the full insertion of z-pins.

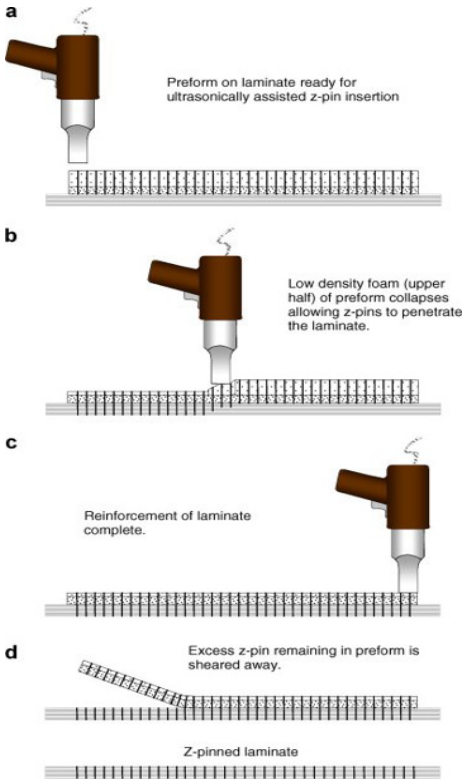

Figure 2: Schematic of the UAZ® process [13]

The use of z-pinning can effectively increase the delamination resistance, impact damage tolerance [15,34,35]. Several researches [14,35–37] have been demonstrated that z-pinning technology can improve the interlaminar fracture toughness under different shear modes (I, II, mixed mode). The ultimate strength and fatigue life of lap joints can be improved using z-pinning [38–40]. In contrast, the in-plane mechanical properties can be reduced due to the insertion of pins through-thickness. This reduction is caused by the microstructural damage, such as fiber crimp and waviness, after the penetration of pins.

The pins not only can reinforce the panels in large areas but also can be used in selective areas requiring local reinforcement. The current application of z-pins for aircrafts is achieved in the *F/A-18E/F Super Hornet*, which are used to replace titanium fasteners in the air inlet ducts and engine bay doors [41]. The composite roll-over bars on Formula 1 racing cars are also reinforced using the z-pinning technique [13].

2.3. Stitching

A successful stitching technique needs cooperation between sewing machine, stitch, needle and thread. Industrial sewing machines are generally used to achieve the penetration of the needle into the fabric layers. Three common types of stitches are illustrated in **Figure 3**, namely lock stitch, modified lock stitch and chain stitch respectively. Lock stitch including a two-thread loop between the needle and the bobbin threads is mainly used in the apparel industry. Two threads are inserted from both the bottom and the top of the laminate. For aesthetic purposes, the intersection of the bobbin and needle threads is concealed in the fabric structure [9]. However, based on the investigation of Morales et al. [42], a high-stress concentration point can be generated due to the thread intersection in the middle of the fabric. Because of this problem, a modified lock stitch with the needle thread stretching on the surface of laminate is achieved by unbalancing the tension between the bobbin and needle threads [42,43]. Furthermore, the third type stitch is known as chain stitch, which is similar to the knitting operation with a single yarn creating a loop around itself [42].

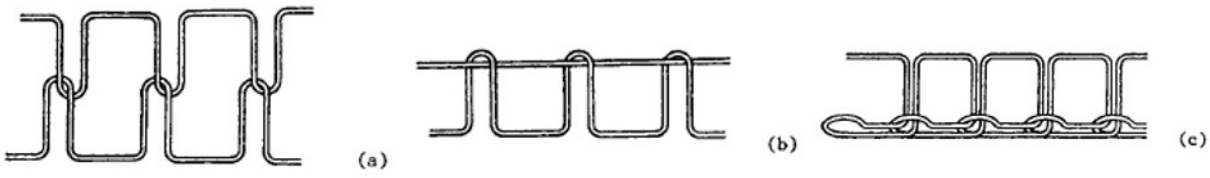

Figure 3: Illustrations of (a) lock stitch (b) modified lock stitch (c) chain stitch [9]

Compared to 2D laminates, the stitched composites have many advantages, such as the improvement of impact damage resistance and post-impact mechanical properties. Many research works [9,44] have shown that there are significant improvements in interlaminar fracture toughness [9,45], fatigue resistance [46] and impact damage resistance [9] for the stitched composite. By changing sewing parameters (stitching density, pattern or stitching

thread), the stitching technique presents a wide range of flexibility in the processing of through-thickness reinforcement. However, a large amount of published mechanical property data reveals that stitching usually reduces the in-plane stiffness, the strength of a laminate by not more than 10-20%, especially in the observation for loading in compression, tension, bending or shear [45]. These changes of in-plane mechanical performances are probably caused by the fiber breakage, misalignment and fiber crimping, as a creation of resin-rich pocket can be generated when the stitching yarns are inserted.

For the application of the stitching technique, stitched composite structures have been widely used as aircraft joints to reduce the number of mechanical fasteners or rivets [47]. The composite structure can be stitched into primary structures, such as T/J section stiffeners [44,48,49], lap joints [48,50–52], angle joints [50] and wing-to-spar joints [44,53]. As a result, the traditional joining methods (riveting, adhesive bonding) in the aircraft industry have been altered dramatically by stitching technique.

2.4. Tufting

In the industrial manufacturing procedure for carpet and warm garments, the tufting technique has been invented and applied at a large scale [54]. Recently, this technique has become commercially available access for achieving through-thickness reinforcement (TTR) in thermosetting polymer matrix composites [55]. It is ideally suitable for load-bearing structures produced by the liquid resin molding process.

As illustrated in Fig.4a [54], a hollow needle as a carrier of additional yarns is inserted into the dry preform through-the-thickness. After the retraction of the needle, the inserted yarns can be retained inside the preform or the underlying support (plasitic/silicone foam or wooden board) due to the friction and form a loop. The loops of tufting yarns are not tied or interlocked, and only a single side of the preform is needed to be accessed, which improves the flexibility in use. In addition, the tufting yarn can be fully inserted with loops on the underside of the structure, or partially inserted to conceal the loops and to avoid the creation of resin pocket **(Figure 4b)**. The feed direction of the needle can be orthogonal or angled to the preform surface **(Figure 4c).** In order to reduce or avoid the frequent thread breakage, the initial selection of a suitable tufting yarn coupled with a suitable selection of the needle eye shape, support and tufting speed should be well considered.

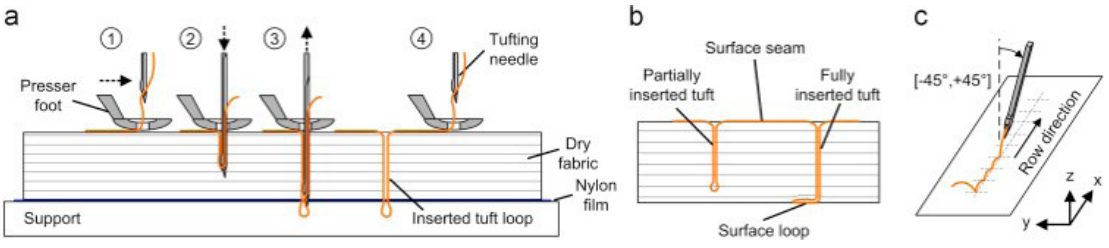

Figure 4: Schematic of the thread arrangement in a tufted preform: (a) details the sequential steps of a full insertion, (b) illustrates the option of partial penetration while (c) shows angled insertion [54].

Comparing with the traditional dual-thread stitching technique, tufting based on a tension-free system can reduce damage to the fabric caused by the sewing effect [56–58]. The requirement of needle access only from one side of the fabric makes this process easier and more efficient. Many researches [37,55,59] have observed that the compression after impact strength and delamination resistance of tufted composites can be much increased, due to the use of tufting yarns. At the same time, a reduction in tensile strength and compressive strength can be found owing to the presence of tufts [55]. An irregular formation of loops can be generated due to a bad selection of support, which can affect the final composite part quality.

Tufting technique can be also applied on the sandwich composite structures with different cores, where the tuft loops are used to bind the composite external layer to the core. In such sandwich composite, the inserted tufts can not only improve the skin/core adhesion but also create a truss-like structure among layers to improve the mechanical performance [60,61]. A practical application of such concept is in the patented products of NidaCore® (France) and Acrosoma® (Belgium)[54].

3. Dry Scale Forming Behaviors

Fiber fabrics (glass, carbon, Kevlar…) can be used as the efficient and reliable reinforcements for thin composite materials. The textile composite structures with complex shapes can be manufactured through the forming process from an initial flat fiber fabric, prior to the Resin-Transfer-Molding (RTM) process [62,63] or prior to resin hardening process [64]. The main question for the forming of dry fabric is whether the given fabric is suitable for the given punch shape. Generally, the strains in the directions of the yarns are small. Thus, angular variations between the warp and weft yarns become the main reason to shape the fabric into a non-developable surface. Owing to the undulation variations of weaving and the interactions between warp and weft yarns, some forming defects (misalignment, gap, slippage of yarns network, buckling, wrinkling… [65–67]) can be developed on the deformed fabric. These defects mentioned above, which can bring negative influences on the performance of the final composite part, may be linked to the forming behaviors to some extent. In order to minimize these forming defects effectively, it is important to perform the characterization on different forming behaviors. The following sections give general definitions for several common forming behaviors often studied at the dry fabric scale.

3.1. Material Draw-In

During forming process, the initially flat fiber fabric is deformed significantly to compensate the punch geometry in space. The material draw-in is an important value to describe the degree of deformation of fabric edges after forming. It can be defined as the amount of material varies in the forming process along the contour from the non-deformed position to the deformed one. For a homogeneous fibrous fabric, the material draw-in is quasi symmetrical in the warp and weft directions. This draw-in value can be influenced prominently by layer

orientation, fabric architecture and initial fabric geometry [5,68–70]. Furthermore, the material draw-in values obtained from the experimental data can be also used as the comparison and validation of a finite element forming simulation model [70,71].

Figure 5 illustrates the material draw-in in the warp and weft directions for the common 3D woven fabrics (LTL, AI, ORT) [5]. These warp interlock fabrics have the similar deformation tendency and are quasi symmetrical in the warp and weft directions. The angular variation of warp and weft yarns occurring in the diagonal direction results in an extension of fabric to offset the forming requirement. On the other hand, the fabric yarns along warp/weft directions are compulsorily retracted to the center owing to their poor strains. The measurement can be extracted from the pictures taken from a central point of view and perpendicular to the surface of the preform, with sufficient distance in order to minimize the shooting errors. The maximum material draw-in value measured at the center point of four sides can represent the magnitude of the edge fluctuation of deformed fabric. It can be observed that **(Figure 5)** the maximum value is slightly higher in the weft direction for the layer to layer and orthogonal warp interlock architectures attributed to the different evolution of warp yarns. In the studies of tufting technique [68,69], it has been demonstrated that the maximum material draw-in of a quasi-isotropic tufted preform can be much reduced along with the increase of tufting density.

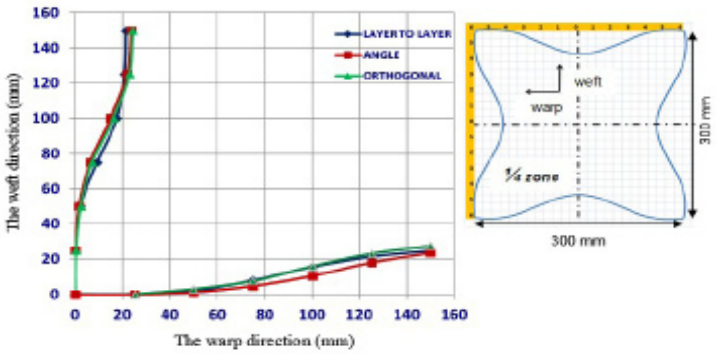

Figure 5: Material draw-in in warp and weft directions (distribution in ¼ zone of the deformed ply) [5].

3.2. Punch force

The measurement of punch force, recorded by a load sensor, can reflect laterally the difficulty of forming for the fabrics. According to the research of Dufour et al. [5], the effort of punch augments rapidly when the 3D woven preforms are being shaped, until the maximum punch displacements have been reached **(Figure 6)**. The punch force drops a bit after achieving the peak value, owing to the inertia effects, and goes back to a constant effort for maintaining the final shape of the deformed preform. Labanieh et al. [72] also have demonstrated that the punch force is closely associated with the initial fabric geometry and layer orientation, during the friction-based blank-holders preforming process. In the study of Liu et al. [68], by comparing the maximum punch force of each tufted sample, it can be concluded that the tufted preforms with higher tufting density become more rigid and need more efforts to be deformed.

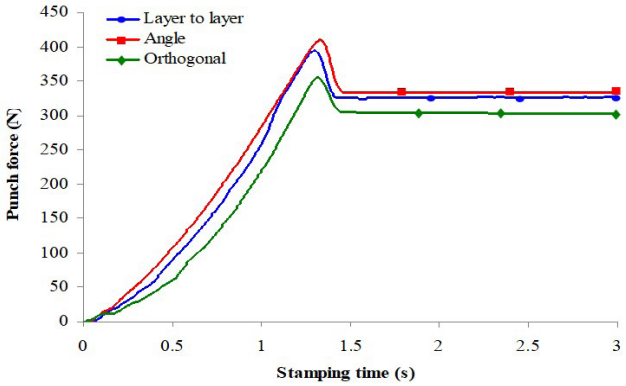

Figure 6: Punch force evolution during the stamping stage for three different warp interlock preforms [5].

3.3. Inter-Layer Sliding

The interlayer sliding is an important phenomenon during the multilayered reinforcement forming process and is the main reason to generate frictions which have a strong effect on the occurrence of defects. Several studies [68,73,74] have observed that the defects are more serious in the forming of multilayered reinforcement with different orientations. It can be explained that if the plies are superimposed in the same directions, they will undergo the same strains during forming and no obvious sliding between plies can be noticed. Therefore, the interlayer sliding is thought to be mainly caused by the different deformation of each ply and slightly influenced by the changed curvature, considering the ply thickness [69].

In some tufting studies [68,69], the maximum interlayer sliding is measured between the top and bottom plies via pictures taken from a central point of view and perpendicular to the surface of the preform. These researches confirmed that higher tufting density can always contribute to smaller sliding among plies. When the tufting density is high enough, it seems that the interlayer sliding can be ignored and the tufted preform deforms as a whole part. Furthermore, VIC3D® stereo-correlation software can be also used to track the white markers plotted on both sides of the reinforcement at the initial state to calculate the sliding between plies at different tracking positions [5,75]. The distance G between the projections on the mid-surface of a pair of measurement points on the opposite surface is considered to be the interlayer sliding value **(Figure 7)** [5]. Consequently, according to different investigations for the through-thickness composite reinforcements, the interlayer sliding can be effectively reduced when the preforms are enhanced in the through-thickness direction.

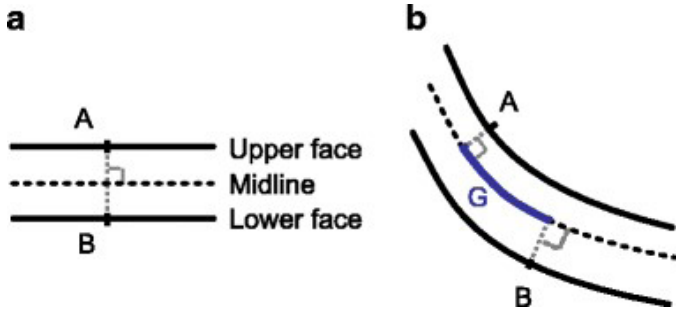

Figure 7: Definition of the sliding G between 2 points A and B, initially opposed on both sides of a composite reinforcement (a) initial state (b) deformed state.

3.4. Shear Angle

Shear angle, which generally refers to the change in the angle between warp and weft yarns during the deformation of woven fibrous reinforcement, is another important forming behavior for the comparison with the numerical output of the model [71,76,77]. As the fabric yarns have very high tensile strength and relatively low transverse strength, the shear angles in different areas of fabric certainly undergo different variations in the final shape after forming. The orientation of fibers has a significant influence on the following resin infusion process and further affects the properties of the final structure. Theoretically, suppose f1a normalized base vector along the first fiber direction and f2 a normalized base vector along the second fiber direction. The in-plane shear angle (radians) is [71]:

$$\gamma = \frac{\pi}{2} - \cos^{-1}\left(\frac{f1 \cdot f2}{||f1|| \cdot ||f2||}\right) \quad (1)$$

A correct and reliable method for the measurement of the shear angle is quite necessary. Recently, an optical full-field strain measurement called digital image correlation (DIC) technology becomes popular and starts to be applied to textile deformability researches [76–79]. With the help of DIC, qualitative and quantitative information on the heterogeneous deformation of an object surface can be obtained. Two CCD cameras (charge-coupled device) are used to take images for the deformed object **(Figure 8)**. A sequence of digital images of a deforming object and a reference image of the object are compared with the use of the image correlation technique. The strains and shear angles can be calculated in the tangential plane of the object from the 3D displacement fields. Though optical measurements can offer quite useful information, they do not describe the forming behavior on the basis of the occurring mechanisms and real forces [17]. An alternative way of the optical camera system is the integration of in situ strain sensors into the textile structure [80–82]. These sensors can be inserted into the fabric with a specific angle to the warp/weft direction. The shear angle can be calculated by the measurement of tensile strain along the sensor. However, when the in situ strain sensors are used, a 10% difference in the shear angles values can be found compared to the data obtained by optical measurement on the surface [81]. It can be attributed to a possible relative slippage of the sensors and the fact that sensors only measured the overall tensile strain along their length [17].

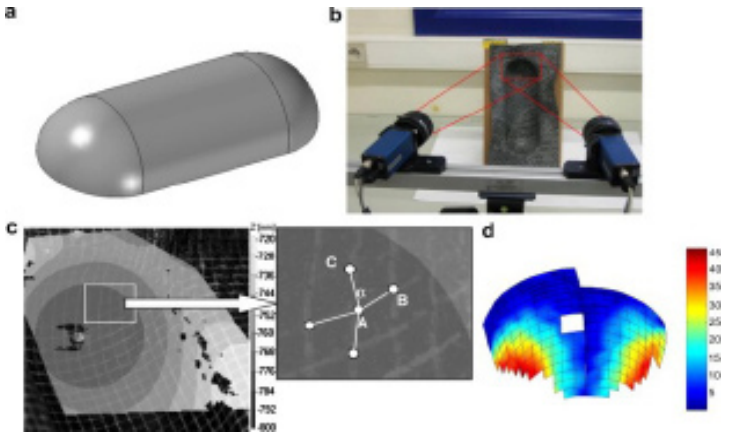

Figure 8: Measurements of the local deformations of the shaped preform: (a) the mold; (b) set-up of DIC; (c) a correlated surface that depicts the z-coordinate of the surface in grey-scale overlaid on a picture of a deformed sheet; (d) calculated shear angle distribution[76].

Molnar et al. [83] have investigated the influence of stitching patterns on the shear behaviors of dry preforms and thermoplastic matrix (PA12) impregnated laminates. Based on their study, the local stitching can influence the overall shear deformation of the laminate. The influence of stitching on the shear angle is relatively lower in the forming of the thermoformed laminate than with dry preform.

3.5. Wrinkling

As the most common defect experienced in the textile composite reinforcement forming process, wrinkles have the ability to degrade the performance of the final product. Wrinkles occur as the energy needed for an out-of-plane deformation is less than that for an in-plane deformation [73]. The out-of-plane deformation depends on the bending stiffness, which is generally weak owing to the fiber property. Several simulation studies[66,84] have proved that the size of wrinkles increases when the bending stiffness of fibrous fabric becomes higher. In the forming of a quasi-isotropic multilayered reinforcement, it is more difficult to avoid the appearance of wrinkles as the relatively serious interlayer sliding can bring in more friction between plies [69,73,74].

Furthermore, a good characterization data of wrinkles in 3D space is quite significant for the evaluation of wrinkling severity and the validation of simulation results. Some image analysis methodologies have been applied to achieve such kind of characterization. Lee et al. [85] quantified the wrinkling level of fibrous fabric preforms by capturing the scattering of the laser light on the wrinkled surface. Although wrinkling contours obtained at a specific height cannot reflect the whole wrinkling severity of samples, the method nevertheless provides a quantitative way to demonstrate the reduction of wrinkling due to the increase of blank holder force. Arnold et al. [86] characterized the wrinkles of non-crimp fabrics during draping by a rig and image analysis methodology. 3D reconstruction of the fabric can be performed from a z-stack of images containing the best degree of focus and the height information for each pixel. According to their characterization of wrinkling, it can be concluded that wrinkle formation

is strongly dependent on the fabric architecture and increases with the augmentation of punch displacement. Shen et al. [87] recently developed a method based on the Structure-From-Motion (SFM) technique to identify wrinkles of the quasi-isotropic tufted fabrics. 3D reconstruction of point-cloud can be established by a full-range image stream taken from all directions of the sample. Then, wrinkling features are extracted by calculating the deviation from a wrinkled shape to a reference shape **(Figure 9)** and analyzed by different indicators to have a general understanding. In this study, they have demonstrated that wrinkle patterns critically depend on the tufting patterns, which should correspond to the punch shape to minimize wrinkling phenomenon.

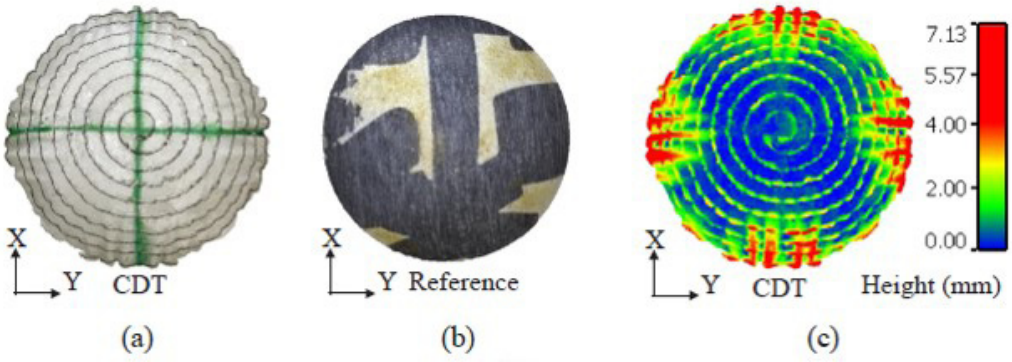

Figure 9: Example of wrinkle characterization methodology, (a) tufted sample model, (b) wrinkle-free sample model, (c) wrinkle pattern [87].

3.6. Buckling

At the scale of the yarns (mesoscale), another common forming defect occurs due to out-of-plane misalignment also called yarn buckles [67,73,88]. These yarn buckles are not in contact anymore with the punch surface and have a strong influence on the resin flow impregnation, because they can modify the pore space and geometry within the fabric. The variation of the in-plane and through-the-thickness permeability can consequently impact the performance of the final composite part [89,90]. The apparition of buckles is the consequence of a specific in-plane bending behavior of yarn subjected to biaxial-tension deformations during the forming process [67]. The difference between the fabric wrinkling phenomenon and yarn buckling phenomenon can be observed in the Fig.10. Although both defect areas have a form of yarn bending, the morphology and scale are different in the two cases. Wrinkling is a fabric-scale strain mode resulting in a classical membrane out-of-plane bending; on the other hand, a “buckle” is a mesoscale (yarn scale) phenomenon that only concerns individual yarns and does not result in any membrane strain [73].

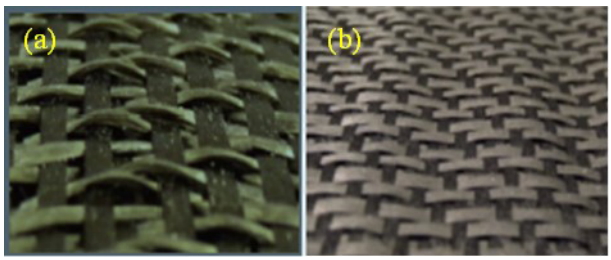

Figure 10: Detail of (a) buckles and (b) wrinkles [73]

Such buckling phenomenon normally occurs in the forming of a highly double-curved and deep-draw shape (tetrahedron, prism and square-box shape), which can generate a wide range of defects with significant amplitudes. With the help of a marks tracking technique [91], for the common 2D composite laminates, Ouagne et al. [67] demonstrated that a reduction of the yarn buckle size can be obtained by increasing the membrane tension. The localization of the buckles strongly depends on the initial orientation of the fabric on the preforming device. In the scale of through-thickness reinforcement, Shen et al. [69] observed that an out-of-plane buckling phenomenon of the inserted tufting yarns appears at the corners of a square-box punch coupled with circle spiral tufting patterns **(Figure 11)**. However, the size of the tufting yarn buckles can be much reduced owing to an increase of tufting density at the corners and these buckles can be eliminated when square spiral tufting patterns are used.

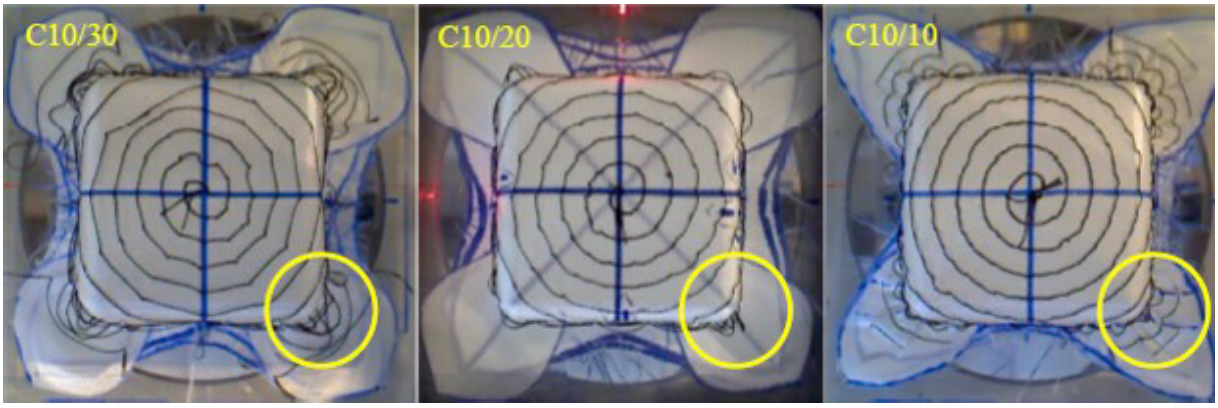

Figure 11: Top view of the deformed preforms with different tufting density [69].

4. Conclusion

Several techniques for manufacturing the through-thickness composite reinforcements as well as the forming behaviors of these structures are reviewed in this chapter. The reinforcement in the through-thickness direction can provide an effective bonding effect among laminated plies, which are sensitive to the delamination. The through-thickness composite reinforcements can significantly improve the delamination resistance and impact damage tolerance, but in-plane fiber damage and the creation of resin pockets can degrade other mechanical properties, such as in-plane tension, compression and shear properties. The extent of mechanical properties and forming behaviors affected by reinforcing techniques is dependent on the reinforcing parameters (density, pattern, yarn tension…). In order to maximize delamination resistance with minimal loss of in-plane mechanical properties and forming defects, an optimal combination of the textile fabric structures and reinforcing parameters is necessary to be identified.

5. References

1. Mouritz AP. Tensile fatigue properties of 3D composites with through-thickness reinforcement. Compos Sci Technol 2008;68:2503–10.

2. Mouritz AP, Bannister MK, Falzon PJ, Leong KH. Review of applications for advanced three-dimensional fibre textile composites. Compos Part A Appl Sci Manuf 1999;30:1445–61.

3. Ansar M, Xinwei W, Chouwei Z. Modeling strategies of 3D woven composites: a review. Compos Struct 2011;93:1947–63.

4. De Luycker E, Morestin F, Boisse P, Marsal D. Simulation of 3D interlock composite preforming. Compos Struct 2009;88:615–23.

5. Dufour C, Wang P, Boussu F, Soulat D. Experimental Investigation About Stamping Behaviour of 3D Warp Interlock Composite Preforms. Appl Compos Mater 2014;21:725–38. doi:10.1007/s10443-013-9369-9.

6. Rudov-Clark S and, Mouritz AP. Tensile fatigue properties of a 3D orthogonal woven composite. Compos Part A Appl Sci Manuf 2008;39:1018–24.

7. Mahadik Y, Brown KAR, Hallett SR. Characterisation of 3D woven composite internal architecture and effect of compaction. Compos Part A Appl Sci Manuf 2010;41:872–80.

8. Baucom JN and, Zikry MA. Low-velocity impact damage progression in woven E-glass composite systems. Compos Part A Appl Sci Manuf 2005;36:658–64.

9. Dransfield K, Baillie C, Mai Y-W. Improving the delamination resistance of CFRP by stitching—a review. Compos Sci Technol 1994;50:305–17.

10. Dransfield K, Baillie C, Mai Y-W. On stitching as a method for improving the delamination resistance of CFRPs. Minerals, Metals and Materials Society, Warrendale, PA (United States); 1993.

11. Bannister M, Herszberg I. Research activities in textile preforms at the Cooperative Research Centre for Aerospace Structures. Int. Aerosp. Congr. 1995 Proceedings; Second Pacific Int. Conf. Aerosp. Technol. Sixth Aust. Aeronaut. Conf., Institution of Engineers, Australia; 1995, p. 619.

12. Crothers PJ, Kruckenberg T, Herszberg I, Bannister MK. Textile processes for the manufacture of composite materials. Int. Aerosp. Congr. 1995 Proceedings; Second Pacific Int. Conf. Aerosp. Technol. Sixth Aust. Aeronaut. Conf., Institution of Engineers, Australia; 1995, p. 531.

13. Mouritz AP. Review of z-pinned composite laminates. Compos Part A Appl Sci Manuf 2007;38:2383–97.

14. Partridge IK, Cartié DDR. Delamination resistant laminates by Z-Fiber® pinning: Part I manufacture and fracture performance. Compos Part A Appl Sci Manuf 2005;36:55–64.

15. Zhang X, Hounslow L, Grassi M. Improvement of low-velocity impact and compression-after-impact performance by z-fibre pinning. Compos Sci Technol 2006;66:2785–94.

16. Gnaba I, Legrand X, Wang P, Soulat D. Literature review of tufted reinforcement for composite structures. IOP Conf Ser Mater Sci Eng 2017;254. doi:10.1088/1757-899X/254/4/042011.

17. Gereke T, Döbrich O, Hübner M, Cherif C. Experimental and computational composite textile reinforcement forming: A review. Compos Part A Appl Sci Manuf 2013;46:1–10. doi:10.1016/j.compositesa.2012.10.004.

18. McClain M, Goering J. Overview of recent developments in 3D structures. Albany Eng Compos 2012:1–12.

19. Khokar N. 3D fabric-forming processes: distinguishing between 2D-weaving, 3D-weaving and an unspecified non-interlacing process. J Text Inst 1996;87:97–106.

20. Chen X, Taylor LW, Tsai L-J. An overview on fabrication of three-dimensional woven textile preforms for composites. Text Res J 2011;81:932–44.

21. Buchanan S, Grigorash A, Archer E, McIlhagger A, Quinn J, Stewart G. Analytical elastic stiffness model for 3D woven orthogonal interlock composites. Compos Sci Technol 2010;70:1597–604.

22. Bilisik K. Multiaxis three dimensional (3D) woven fabric. Adv Mod Woven Fabr Technol 2011:79–106.

23. El-Dessouky HM, Saleh MN. 3D Woven Composites: From Weaving to Manufacturing. Recent Dev F Carbon Fibers 2018:51.

24. Saleh MN, Soutis C. Recent advancements in mechanical characterisation of 3D woven composites. Mech Adv Mater Mod Process 2017;3:12.

25. Mouritz AP, Baini C, Herszberg I. Mode I interlaminar fracture toughness properties of advanced textile fibreglass composites. Compos Part A Appl Sci Manuf 1999;30:859–70.

26. Lefebvre M, Francois B, Daniel C. Influence of high-performance yarns degradation inside three-dimensional warp interlock fabric. J Ind Text 2013;42:475–88.

27. Hu J. 3-D fibrous assemblies: properties, applications and modelling of three-dimensional textile structures. Elsevier; 2008.

28. McHugh C. Creating 3-D, One Piece, Woven Carbon Preforms Using Conventional Weaving and Shedding. SAMPE J 2009;45:33–41.

29. McHugh C. The Manufacture of One Piece Woven Three Dimensional Carbon Fiber Nodal Structures. SAMPE Conf, 2010.

30. Redman C, Bayraktar H, Mcclain M. Curved beam test Behavior of 3D woven composites. SAMPE Seattle, WA 2014.

31. Bayraktar H, Ehrlich D, Goering J, Mcclain M, Hampshire N. 3D woven composites for energy absorbing. 20th Int. Conf. Compos. Mater. Copenhagen, 2015, p. 19–24.

32. El-Dessouky H, Snape A, Scaife R, Tew H, Modi DK, Kendall K, et al. Design, weaving and manufacture of a large 3D composite structures for automotive applications. 7th World Conf. 3D Fabr. their Appl., vol. 1, Jouve; 2016, p. 123–32.

33. Hemrick JG, Lara-Curzio E, Loveland ER, Sharp KW, Schartow R. Woven graphite fiber structures for use in ultra-light weight heat exchangers. Carbon N Y 2011;49:4820–9.

34. Partridge I, Cartie DDR, Bonnington T. Manufacture and performance of z-pinned composites. Adv Polym Compos 2003.

35. Freitas G, Magee C, Dardzinski P, Fusco T. Fiber insertion process for improved damage tolerance in aircraft laminates. J Adv Mater 1994;25:36–43.

36. Cartié DDR, Partridge IK. Delamination behaviour of Z-pinned laminates. Eur. Struct. Integr. Soc., vol. 27, Elsevier; 2000, p. 27–36.

37. Cartié DDR, Dell'Anno G, Poulin E, Partridge IK. 3D reinforcement of stiffener-to-skin T-joints by Z-pinning and tufting. Eng Fract Mech 2006;73:2532–40. doi:10.1016/j.engfracmech.2006.06.012.

38. Freitas G, Fusco T, Campbell T, Harris J, Rosenberg S. Z-fiber technology and products for enhancing composite design. AGARD Conf. Proc. AGARD CP, 1997, p. 17.

39. Rugg KL, Cox BN, Ward KE, Sherrick GO. Damage mechanisms for angled through-thickness rod reinforcement in carbon–epoxy laminates. Compos Part A Appl Sci Manuf 1998;29:1603–13.

40. Chang P, Mouritz AP, Cox BN. Properties and failure mechanisms of pinned composite lap joints in monotonic and cyclic tension. Compos Sci Technol 2006;66:2163–76.

41. Anon LK. Z-Pins strengthen the Super Hornet, save weight and cost. Integr 2001;3:1–2.

42. Morales A. Structural stitching of textile preforms. Adv Mater Look Ahead to 21 St Century 1990:1217–30.

43. Ogo Y. The effect of stitching on in-plane and interlaminar properties of carbon-epoxy fabric laminates 1987.

44. Mouritz AP, Jain LK. Further validation of the Jain and Mai models for interlaminar fracture of stitched composites. Compos Sci Technol 1999;59:1653–62.

45. Mouritz AP, Cox BN. A mechanistic approach to the properties of stitched laminates. Compos Part A Appl Sci Manuf 2000;31:1–27.

46. Aymerich F, Priolo P, Sun CT. Static and fatigue behaviour of stitched graphite/epoxy composite laminates. Compos Sci Technol 2003;63:907–17.

47. Rispler AR. Analysis and optimisation of highly loaded joints 1998.

48. Sawyer JW. Effect of stitching on the strength of bonded composite single lap joints. AIAA J 1985;23:1744–8.

49. Mitchell LR, Herszberg I. Analysis and testing of stitched stiffened carbon/epoxy shear panels. Int. Aerosp. Congr. 1995 Proceedings; Second Pacific Int. Conf. Aerosp. Technol. Sixth Aust. Aeronaut. Conf., Institution of Engineers, Australia; 1995, p. 593.

50. Tada Y, Ishikawa T. Experimental evaluation of the effects of stitching on CFRP laminate specimens with various shapes and loadings. Key Eng. Mater., vol. 37, Trans Tech Publ; 1989, p. 305–16.

51. Tong L, Jain LK, Leong KH, Kelly D, Herszberg I. Failure of transversely stitched RTM lap joints. Compos Sci Technol 1998;58:221–7.

52. Tong L, Jain LK. Analysis of adhesive bonded composite lap joints with transverse stitching. Appl Compos Mater 1996;2:343–65.

53. Whiteside JB, DeIasi RJ, Schulte RL. Measurement of preferential moisture ingress in composite wing/spar joints. Compos Sci Technol 1985;24:123–45.

54. Dell'Anno G, Treiber JWG, Partridge IK. Manufacturing of composite parts reinforced through-thickness by tufting. Robot Comput Integr Manuf 2016;37:262–72. doi:10.1016/j.rcim.2015.04.004.

55. Dell'Anno G, Cartié DD, Partridge IK, Rezai A. Exploring mechanical property balance in tufted carbon fabric/epoxy composites. Compos Part A Appl Sci Manuf 2007;38:2366–73. doi:10.1016/j.compositesa.2007.06.004.

56. Henao A, Carrera M, Miravete A, Castejón L. Mechanical performance of through-thickness tufted sandwich structures. Compos Struct 2010;92:2052–9. doi:10.1016/j.compstruct.2009.11.005.

57. Sickinger C, Herrmann A. Structural stitching as a method to design high-performance composites in future. Proc. TechTextil Symp., vol. 2001, 2001.

58. Pérès P, Desmars B, Léard JP. Composite behavior of assemblies with AEROTISS® 03S technology. 16th Int. Conf. Compos. Mater., 2007.

59. Colin de Verdiere M, Pickett AK, Skordos AA, Witzel V. Effect of tufting on the response of non crimp fabric composites. 2007.

60. Henao A, Carrera M, Miravete A, Castejón L. Mechanical performance of through-thickness tufted sandwich structures. Compos Struct 2010;92:2052–9.

61. Potluri P and, Kusak E, Reddy TY. Novel stitch-bonded sandwich composite structures. Compos Struct 2003;59:251–9.

62. Rudd CD, Long AC. Liquid Molding Technologies, Cambridge: Woodhead Pub 1997.

63. Šimáček P, Advani SG. Desirable features in mold filling simulations for liquid composite molding processes. Polym

Compos 2004;25:355–67. doi:10.1002/pc.20029.

64. Blanlot R, Billoet J-L, Gachon H. Study of Non-Polymerised Prepreg Fabrics in“ Off-Axes” Tests. ICCM/9 Compos Des 1993;4:576–83.

65. Potter K, Khan B, Wisnom M, Bell T, Stevens J. Variability, fibre waviness and misalignment in the determination of the properties of composite materials and structures. Compos Part A Appl Sci Manuf 2008;39:1343–54.

66. Boisse P, Hamila N, Vidal-Sallé E, Dumont F. Simulation of wrinkling during textile composite reinforcement forming. Influence of tensile, in-plane shear and bending stiffnesses. Compos Sci Technol 2011;71:683–92. doi:10.1016/j.compscitech.2011.01.011.

67. Ouagne P, Soulat D, Moothoo J, Capelle E, Gueret S. Complex shape forming of a flax woven fabric; analysis of the tow buckling and misalignment defect. Compos Part A Appl Sci Manuf 2013;51:1–10.

68. Liu LS, Zhang T, Wang P, Legrand X, Soulat D. Influence of the tufting yarns on formability of tufted 3-Dimensional composite reinforcement. Compos Part A Appl Sci Manuf 2015;78:403–11. doi:10.1016/j.compositesa.2015.07.014.

69. Shen H, Wang P, Legrand X, Liu L, Soulat D. Influence of the tufting pattern on the formability of tufted multi-layered preforms. Compos Struct 2019;228:111356.

70. Nasri M, Garnier C, Abbassi F, Labanieh AR, Dalverny O, Zghal A. Hybrid approach for woven fabric modelling based on discrete hypoelastic behaviour and experimental validation. Compos Struct 2019;209:992–1004.

71. Khan MA, Mabrouki T, Vidal-Sallé E, Boisse P. Numerical and experimental analyses of woven composite reinforcement forming using a hypoelastic behaviour. Application to the double dome benchmark. J Mater Process Technol 2010;210:378–88. doi:10.1016/j.jmatprotec.2009.09.027.

72. Labanieh AR, Garnier C, Ouagne P, Dalverny O, Soulat D. Intra-ply yarn sliding defect in hemisphere preforming of a woven preform. Compos Part A Appl Sci Manuf 2018;107:432–46. doi:10.1016/j.compositesa.2018.01.018.

73. Allaoui S, Cellard C, Hivet G. Effect of inter-ply sliding on the quality of multilayer interlock dry fabric preforms. Compos Part A Appl Sci Manuf 2015;68:336–45. doi:10.1016/j.compositesa.2014.10.017.

74. Vanclooster K, Lomov S V, Verpoest I. On the formability of multi-layered fabric composites. Proc 17th Int Conf Compos Mater 2009:1–10.

75. Bel S, Boisse P, Dumont F. Analyses of the deformation mechanisms of non-crimp fabric composite reinforcements during preforming. Appl Compos Mater 2012;19:513–28.

76. Lomov S V, Boisse P, Deluycker E, Morestin F, Vanclooster K, Vandepitte D, et al. Full-field strain measurements in textile deformability studies. Compos Part A Appl Sci Manuf 2008;39:1232–44.

77. Pazmino J, Carvelli V, Lomov S V. Formability of a non-crimp 3D orthogonal weave E-glass composite reinforcement. Compos Part A Appl Sci Manuf 2014;61:76–83.

78. Willems A, Vandepitte D, Lomov SV, Verpoest I. Biaxial tensile tests on a woven glass/PP fabric under optical strain measurement. Proc. 8th Eur. Sci. Assoc. Mater. Form. Conf. Mater. Form., 2005, p. 1004–10.

79. Hivet G, Dumont F, Launay J, Maurel V, Vacher P, Boisse P. Optical analysis of woven fabric’s shear behaviour, 2004.

80. Zhang H, Tao X, Yu T, Wang S. Conductive knitted fabric as large-strain gauge under high temperature. Sensors Actuators A Phys 2006;126:129–40.

81. Zhu B, Yu TX, Zhang H, Tao XM. Experimental investigation of formability of commingled woven composite preform in stamping operation. Compos Part B Eng 2011;42:289–95.

82. Hasan MMB, Matthes A, Schneider P, Cherif C. Application of carbon filament (CF) for structural health monitoring of textile reinforced thermoplastic composites. Mater Technol 2011;26:128–34.

83. Molnar P, Ogale A, Lahr R, Mitschang P. Influence of drapability by using stitching technology to reduce fabric deformation and shear during thermoforming. Compos Sci Technol 2007;67:3386–93.

84. Liang B, Hamila N, Peillon M, Boisse P. Analysis of thermoplastic prepreg bending stiffness during manufacturing and of its influence on wrinkling simulations. Compos Part A Appl Sci Manuf 2014;67:111–22. doi:10.1016/j.compositesa.2014.08.020.

85. Lee JS, Hong SJ, Yu W-R, Kang TJ. The effect of blank holder force on the stamp forming behavior of non-crimp fabric with a chain stitch. Compos Sci Technol 2007;67:357–66.

86. Arnold SE, Sutcliffe MPF, Oram WLA. Composites : Part A Experimental measurement of wrinkle formation during draping of non- crimp fabric. Compos PART A 2016;82:159–69. doi:10.1016/j.compositesa.2015.12.011.

87. Shen H, Wang P, Legrand X, Liu L. Characterisation and optimisation of wrinkling during the forming of tufted three-dimensional composite preforms 2019.

88. Capelle E, Ouagne P, Soulat D, Duriatti D. Complex shape forming of flax woven fabrics: Design of specific blank-holder shapes to prevent defects. Compos Part B Eng 2014;62:29–36.

89. Lee SH, Han JH, Kim SY, Youn JR, Song YS. Compression and relaxation behavior of dry fiber preforms for resin transfer molding. J Compos Mater 2010;44:1801–20.

90. Skordos AA, Aceves CM, Sutcliffe MPF. A simplified rate dependent model of forming and wrinkling of pre-impregnated woven composites. Compos Part A Appl Sci Manuf 2007;38:1318–30.

91. Bretagne N, Valle V, Dupré JC. Development of the marks tracking technique for strain field and volume variation measurements. NDT E Int 2005;38:290–8.